Control Systems Analysis and Design

Article I

Jessé de Oliveira Santana Alves

October, 2021

Contents

1 Internal Model Principle

1.1 Motivation

In a control project, there are basic concerns such as: stability, reference tracking, regulation and sensitivity. To achieve this, different control techniques and conceptual and mathematical analyzes can be implemented to solve these problems and also meet performance criteria in physical systems. In this challenge, the conceptual proposition called the Internal Model Principle will be used to solve the problems of Reference Tracking and Regulation.

This proposition seeks in a conceptual way - thus replacing formal algebraic analysis - to analyze the response in a steady state, aiming to reject persistent disturbances at the plant's entrance and exit. This type of analysis proves to be very effective, since theoretical analysis brings faster conclusions than algebraic development, in addition to most of the control problems being in following references and rejecting disturbances. Especially in industries, the rejection of disturbances is often more desired than the following of references, as these do not usually change during the process, and the greatest concern is to prevent persistent oscillations from hindering production. A good example of this is in industrial tank level controls, which are designed to operate at certain fixed heights - whether for temperature control, concentration, among others - and the emergence of disturbances in the valves or inlet or outlet need to be compensated. by the controller.

1.2 Simulations performed

For this challenge, given the system na Figure 1 below, the following simulations were performed:

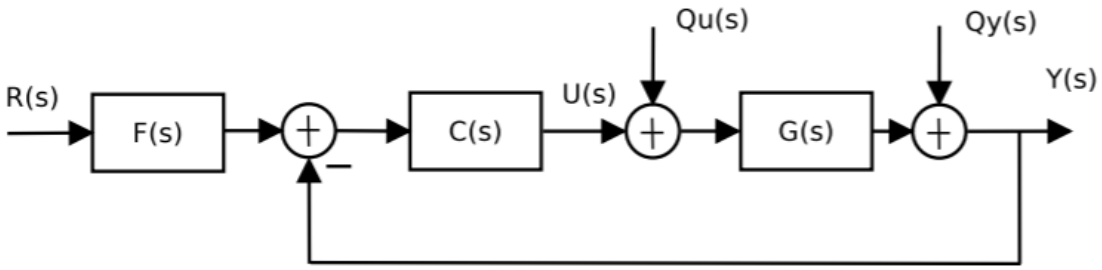

Figure 1: Control System with Reference Filter for Challenge I

1. Using the plant $G(s) = \frac{2}{s}$, a proportional gain controller K was designed that provides a settling time of 2% for change reference to the unit step is equal to 4s, with this reference changing every 2 seconds. In this first case, the reference filter was considered unitary and the step-type disturbances were: $Q_u(s) = -0.2\frac{e^{-25s}}{s}$ and $Q_y(s) = -0.2\frac{e^{-15s}}{s}$. For this first item, as the closed-loop system is of first order, model represented in Equation 1, the control was reduced to: Using Equation 2, which describes the time for 98% of the answer, make $t_s = 4s$ and therefore determine a $\tau = 1$.

$$G(s) = \frac{C}{\tau s + 1} \tag{1}$$

$$t_s = 4\tau \tag{2}$$

Then, take the closed-loop transfer function below:

$$FT_{MF}(s) = \frac{2K}{s + 2K}$$

And put it in the format Equation 1:

$$FT_{MF}(s) = \frac{1}{\frac{1}{2K}s + 1} \tag{3}$$

And then, comparing the first term of the polynomial in the denominator of Equations 1 and 3, we have that:

$$\tau = \frac{1}{2K}$$

Since $\tau = 1$, consequently:

$$K = 0.5$$

2. In the second simulation, the plant remained the same $G(s) = \frac{2}{s}$, however the designed controller was a PI with $C(s) = K\frac{s+z}{s}$, whose objective was to allocate two poles of the closed loop $1 + C(s)G(s)$ at -1. Subsequently, the reference filter $F(s) = \frac{\tau_n s+1}{\tau_d s+1}$ should make the output have a settling time of e 2% for reference change the step is equal to 6s. To do this, a comparison of polynomials was made between the characteristic polynomial $1 + C(s)G(s)$ described in Equation 4 and the polynomial in Equation 5, whose roots are doubles at -1:

$$s^2 + 2Ks + 2Kz \tag{4}$$

$$s^2 + 2s + 1 \tag{5}$$

Comparing terms:

$$2Ks = 2s \tag{6}$$

$$2Kz = 1 \tag{7}$$

Finally, the gain and zero value of the controller were determined. Once the poles were allocated, the reference filter pole was used to eliminate the controller zero, thus avoiding an unwanted overshoot, and the filter zero was chosen in such a way as to achieve a settling time $t_s = 6s$.

However, two situations were considered in the simulation, in the first the disturbances are the same as those described in item 1 above, and in the second, the system was simulated for two ramp-type disturbances , being $Q_u(s) = -0.2\frac{e^{-25s}}{s^2}$ and $Q_y(s) = -0.2\frac{e^{-15s}}{s^2}$.

3. In the third case, the only difference for item 2 is that instead of a project to directly allocate the poles, the parameters $K, z, \tau_n and \tau_d$ were determined in order to guarantee a settling time of 2% for change of reference to the step is equal to 3s. Furthermore, only ramp-type disturbances were simulated : $Q_u(s) = -0.2\frac{e^{-25s}}{s^2}$ and $Q_y(s) = -0,2\frac{e^{-15s}}{s^2}$. Despite the discreet change in the project specification, the strategy for implementation has changed.

Equation 4 was used to determine the settling time in 3s, as follows: For the criterion of 2% we have:

$$t_s = \frac{4}{\xi\omega_n} \tag{8}$$

Therefore, for $t_s = 3s$:

$$\xi\omega_n = \frac{4}{3} \tag{9}$$

Arbitrating a damping coefficient $\xi = 1$, in order to avoid an overshoot, we have a natural frequency $\omega_n = \frac{4}{3}$. So, substituting 9 in Equation 10 and comparing with the polynomial of Equation 4, we obtain a gain $K = \frac{4}{3}$. Subsequently, comparing the third term of Equation 10 with the third term of Equation 4 we obtain a zero for the controller $z = \frac{2}{3}$

$$s^2 + 2\xi\omega_n s + \omega_n^2 \tag{10}$$

Once the PI controller parameters were defined, the following adjustments were made to the reference filter: The filter pole was placed above the controller zero to avoid the overshoot caused by it, therefore $\tau_d = \frac{2}{3}$. Once this was done, the zero of the filter had to be allocated in order to meet $t_s = 3s$, so with trial and error an acceptable value of $\tau_n = 0.73$ was reached .

4. Finally, in the last case the plant changed to $G(s) = \frac{2}{s+1.5}$, the controller continued to be a PI and the reference filter remained unity. As a specification, K and z were designed to meet a t_s of 2% for a change of reference to the step equal to 2s. In this problem three configurations were made: the first with step-type disturbances, the second with sinusoid-type disturbances and the third and last with sinusoidal-type disturbances but with an increase in the PI controller, leaving $C(s) = K == zzfracs + zs\frac{s^2+0.5s+1.8^2}{s^2+2^2}$.

   For the PI project, the procedure was similar to that in item 3. Where through Equation 8, in this case with $t_s = 2s$, the term was determined:

$$\xi\omega_n = 2 \tag{11}$$

   $xi = 1$ was determined to avoid overshoot and consequently ω was equal to 2. Then, with the same process of comparing the polynomials, a gain $K = 1wasobtained.25$ and a zero $z = 1.6$, where z was set to 1.35 to obtain the desired settling time.

1.3 Results obtained

For **first case**, with a proportional gain controller $K = 0.5$, a settling time was obtained:

$$t_s = 3.9121s$$

And given the signs of disturbance from Figure 2:

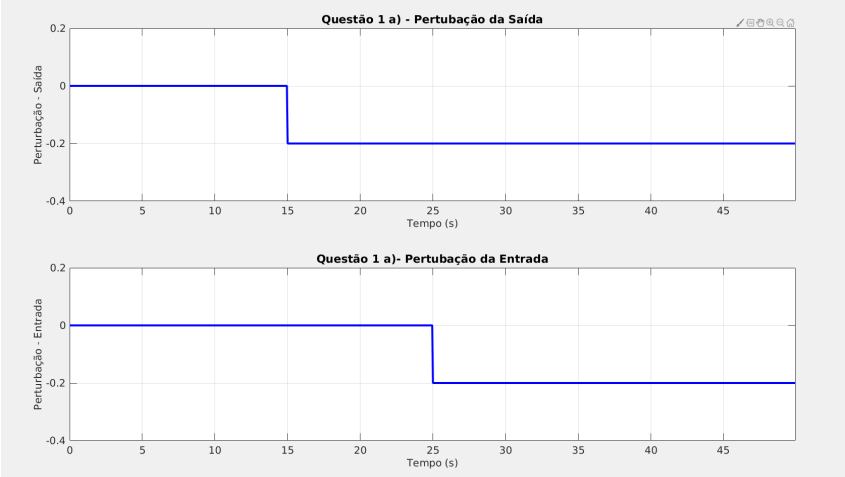

Figure 2: Step-Type Disturbance Signals

An output and control signal was obtained below:

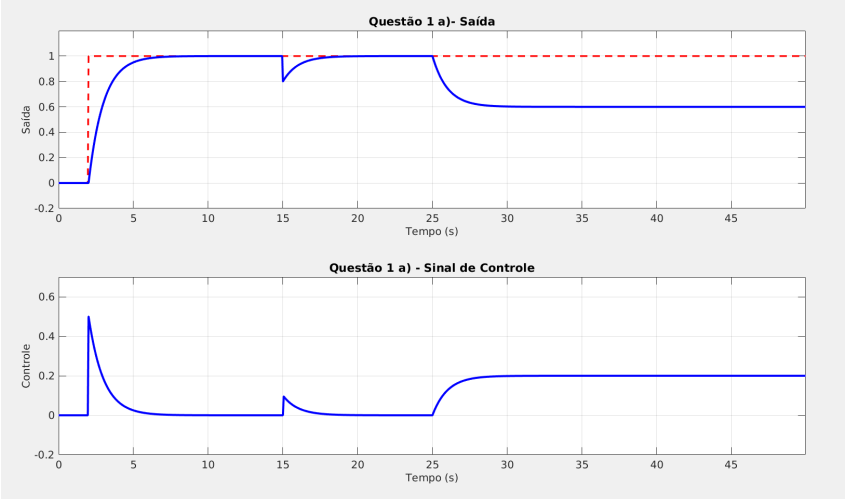

Figure 3: Output and Control Signal for Case 1

Analyzing the Figures 2 and 3, it can be seen that the system managed to reject the disturbance at the output well, however the disturbance at the input caused an *offset* equal to -0.2 which is precisely the gain from the disturbance . The Internal Model Principle explains this fact as follows: In order for the disturbance to be rejected by the controller, it is necessary that the disturbance model appears internally as poles in the feedback path between the output and the emergence of the disturbance. Following this principle, it is observed that for output disturbance , both the controller poles and the plant poles can cancel the disturbance, as long as they are the same. However, for input disturbance , only the controller poles are capable of eliminating the disturbance.

And this is precisely what happens in the first case, as the plant $G(s)$ has an integrator, which cancels the output disturbance , which is of the step type. However, in the case of the input disturbance , which is also of the step type, only the controller could eliminate it, and this only consists of a proportional gain K, which is why it was not rejected.= = zz

For **second case**, we obtained a PI controller:

$$C(s) = 1\frac{s + 0.5}{s} \tag{12}$$

And a reference filter given by:

$$F(s) = \frac{-0.2s + 1}{2s + 1} \tag{13}$$

Where the zero of the reference filter was placed in the SPD to achieve the settling time criterion, reaching a result of:

$$t_s = 6.0012s$$

Furthermore, two types of disturbances were considered, first of the step type and later of the ramp type. For the step type we have a disturbance equal to the first case, shown in Figure 2, while the output and control signal is shown below in Figure 4.

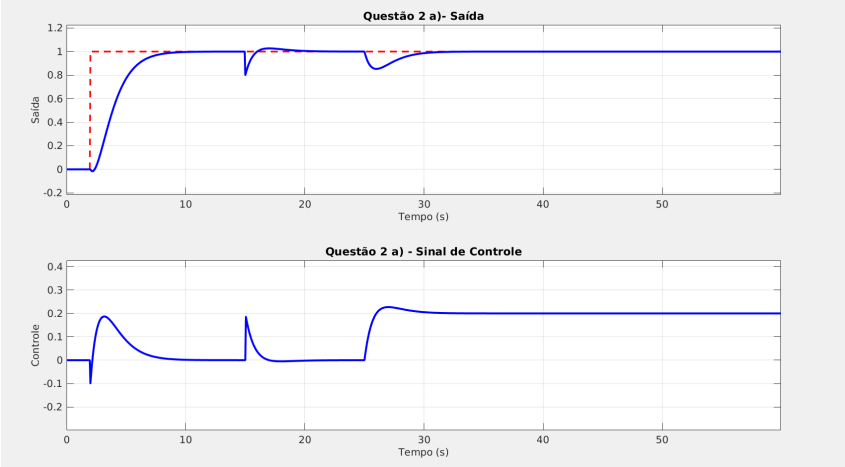

Figure 4: Output and Control Signal for Case 2

It can be seen in Figure 4 that the system was able to reject the two disturbances , since according to the description above of the Internal Model Principle, the controller is of the PI type - therefore it has an integrator - and the disturbances are of the type step.

When the disturbance changes to the ramp type, shown in Figure 5, we notice the same *offset* of -0.4 in the output signal when the input disturbance Figure 6 occurs.

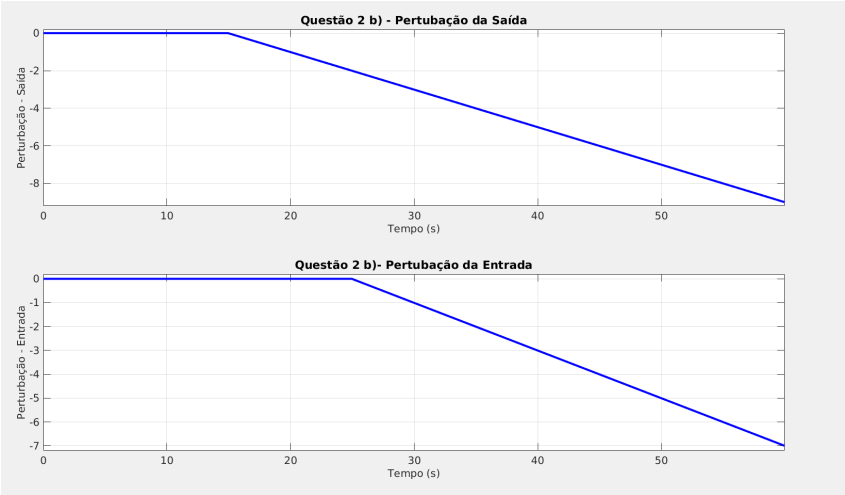

Figure 5: Ramp Type Disturbance

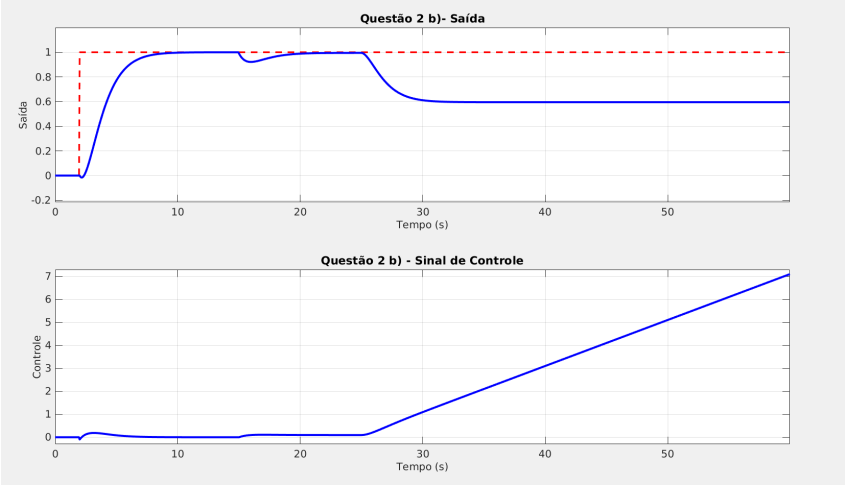

Figure 6: Output and Control Signal for Case 2 with Ramp Type Disturbances

Again, conceptually, it is observed that the PI integrator together with the plan integrator are capable of rejecting the disturbance at the output, but the same does not occur with the disturbance at the input, since the plant poles are unable to interfere.= = zz

In **third case**, we obtained a PI controller given by:

$$C(s) = \frac{4}{3}\frac{s + \frac{2}{3}}{s} \tag{14}$$

And a reference filter given by:

$$F(s) = \frac{0.73s + 1}{1.5s + 1} \tag{15}$$

Producing a settling time:

$$t_s = 3.0110s$$

The perturbation was also of the ramp type, Figure 5, and produced the following output, this time with *offset* of -0.225, and control signal:

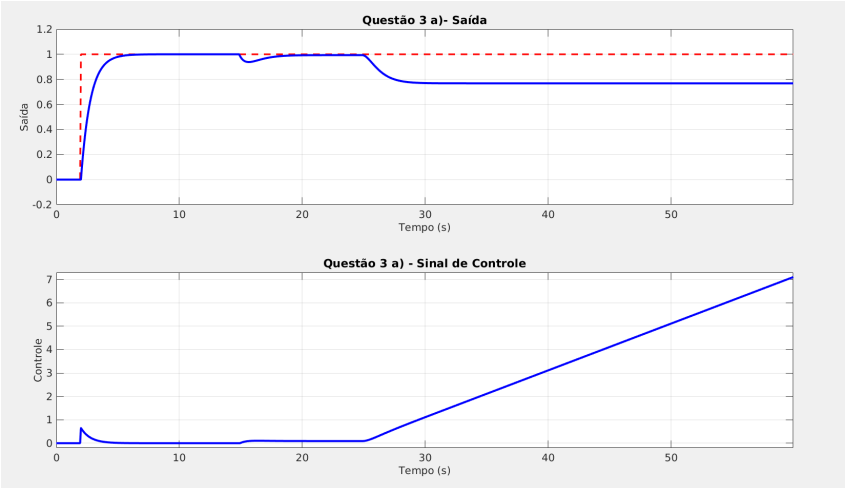

Figure 7: Output and Control Signal for Case 3 with Ramp Type Disturbances

When comparing the figures 4 and 7 it is seen that in both the input disturbance was not rejected, only the value of *offset* varied. This result can be predicted if the simulation is required in two different ways. Firstly conceptually, through the Internal Model Principle, as already described on page 6. Where the feedback path of the output disturbance has only one controller integrator, for this reason it was not possible to eliminate the ramp-type disturbance. Furthermore, algebraically, when the Final Value Theorem between the output $Y(s)$ and the input perturbation $Q_u(s)$ is applied to cases 2 and 3, Equation 10

$$\lim_{t\to\infty} y(t) = \lim_{s\to 0} s\frac{G(s)}{1+C(s)G(s)}Q_u(s) \tag{16}$$

The following result is obtained:

$$\lim_{t\to\infty} y(t) = \frac{-0,4}{2Kz}$$

Therefore, it can be seen that the *offset* discussed above will only be zero if $K \to \infty$, which is not physically viable. Therefore, for case 2, with $K = 1$ and $z = 0.5$ we have:

$$\lim_{t\to\infty} y(t) = -0.400$$

And for case 3, with $K = \frac{4}{3}$ and $z = \frac{2}{3}$ we have:

$$\lim_{t\to\infty} y(t) = -0.225$$

Finally, in **fourth case** we obtained a PI controller equal to:

$$C(s) = 1.25\frac{s+1.35}{s} \tag{17}$$

And a Unitary reference filter:

$$F(s) = 1$$

Producing a settling time of:

$$t_s = 1.9804s$$

And the simulations were carried out in three stages. In the first, step-type perturbation of Figure 8 was applied to the system, producing a result of Figure 9.

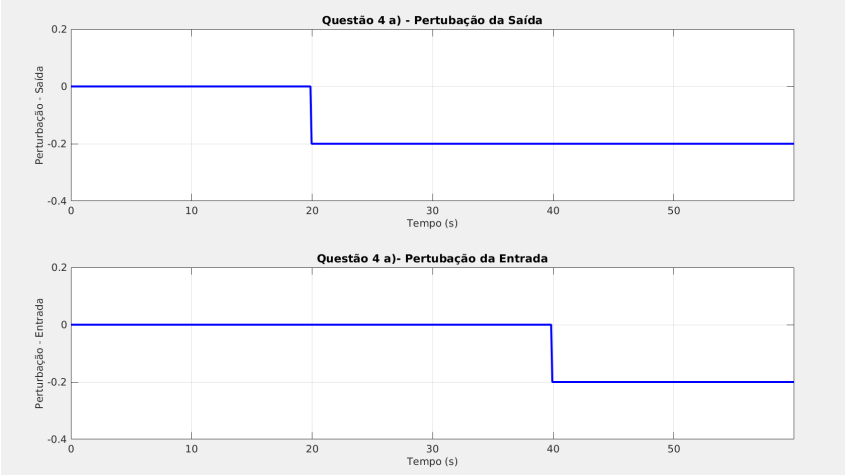

Figure 8: Case 4 Step Type Disturbance

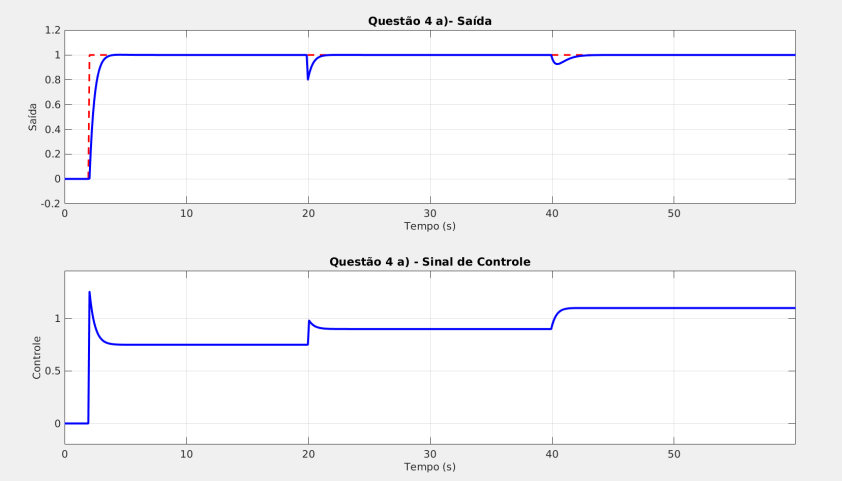

Figure 9: Output and Control Signal for Case 4 with Step Type Disturbances

Again, as in case 2 a), the system rejected the two step-type disturbances due to the PI controller integrator. In the second stage, a sinusoidal disturbance , = = zzautorefq4bp, was applied to both the input and the output, producing the following result Figure 11.

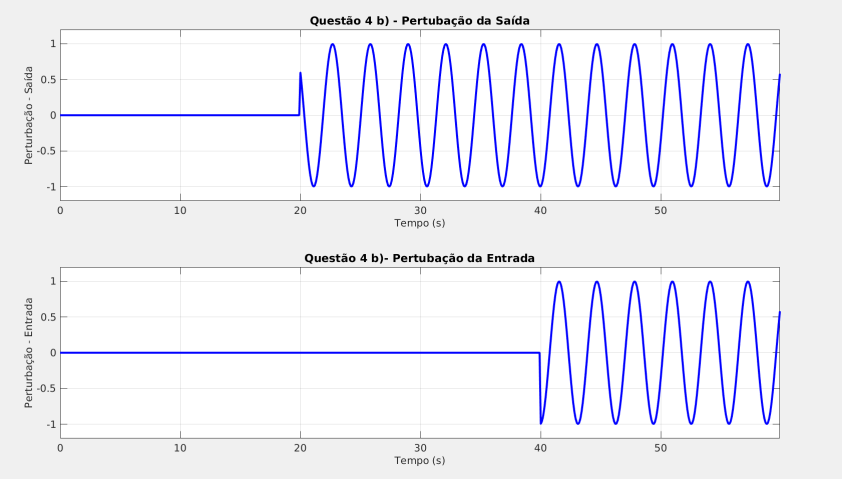

Figure 10: Sinusoidal Type Perturbation

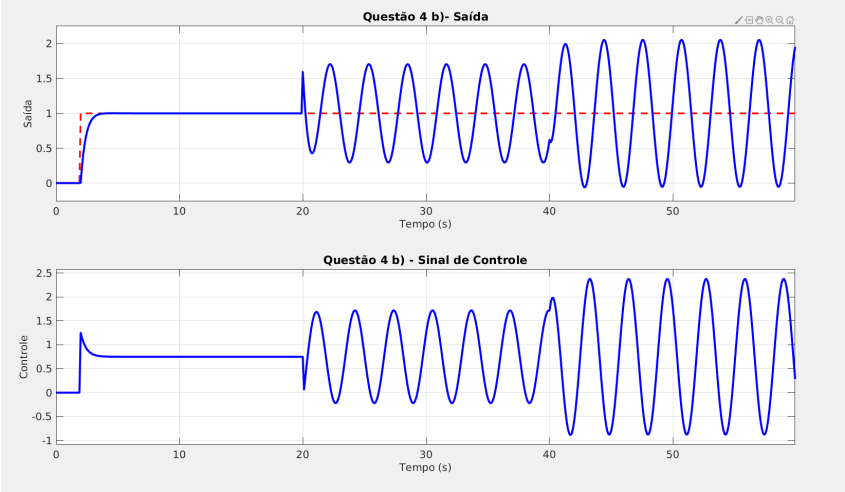

Figure 11: Output and Control Signal for Case 4 with Sinusoidal Type Pertubations

Here it is clear that the system was not able to reject any of the disturbances . Which was already expected conceptually, since sinusoidal modes do not appear in the controller. And in order to prove this, the third and final step was to replace the Equation 17 controller with the controller below:

$$C(s) = 1.25\frac{s+1.35}{s}\frac{s^2+0.5s+1.8^2}{s^2+2^2} \tag{18}$$

When this modification was made, the frequency sinusoid modes $\omega = 2$ were added to the controller, making it possible to reject the disturbance at both the input and output, Figure 12.

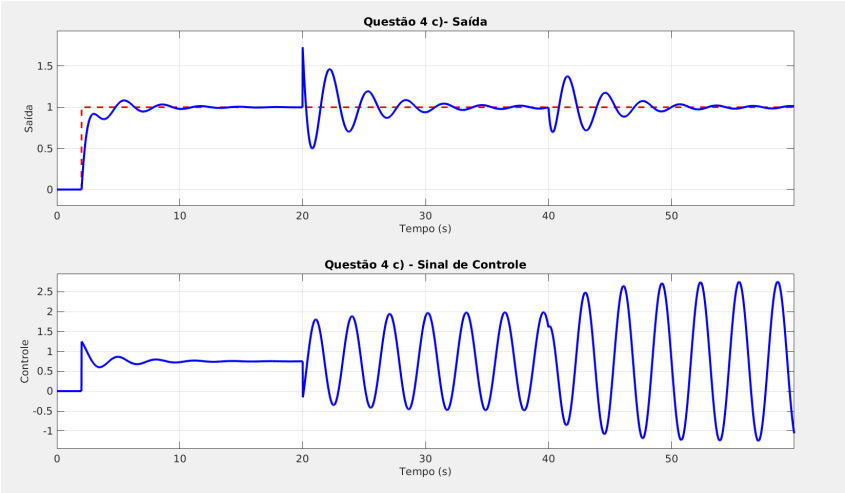

Figure 12: Output and Control Signal for Case 4 with Sinusoidal Type Pertubations

1.4 Conclusions

After analyzing all the simulations, it was possible to see how effective the conceptual proposition of the Internal Model Principle is, as it allows conclusions to be drawn about the influence of input and output disturbances on the system's output signal just by observing the transfer functions $C(s)$,$G(s)$,$Q_u(s)$ and $Q_y(s)$. This theoretical tool, in addition to deepening knowledge about feedback controls, speeds up the analysis process, often depending on what you want to see, dispensing with algebraic developments and computer simulations.

2 Small Gain Theorem and Anti-Windup

2.1 Motivation

The practice of a control project reveals obstacles that need to be overcome with different techniques. This second challenge basically presents three problems present in control projects and their respective corrective tools. The first is in the identification of the systems that will be controlled. Methods such as step response analysis of a process, for example, are used to model plants. However, real systems undergo changes in their structures and therefore in the parameters of their mathematical modeling. So how can you ensure that a designed control will satisfy this system with a family of equations that describe its behavior? To achieve this, robust control techniques are implemented to meet these changes in parameters. In the present work, the small gain theorem will be applied as a way to solve this robust control problem. In this theorem, the condition for robust stability is to ensure that **??** is met:

$$||\mathcal{C}(j\omega) == zzDelta_m(j\omega)||_\infty < 1 \tag{19}$$

Where $\mathcal{C}(j\omega)$ is the complementary sensitivity function given by $\mathcal{C}(j\omega) = \frac{G(j\omega)C(j\omega)}{1+G(j\omega)C(j\omega)}$, with $G(j\omega)$ being the system plan and $C(j\omega)$ the controller, and $\Delta_m(j\omega)$ is the multiplicative uncertainty limit.

The second problem lies in the effect that the abrupt change of reference causes in the system, for example a step input, where there is a jump in the input value, which causes a jump in the error value, also providing a high initial control signal. which can cause an unwanted overshoot at the system output. One of the causes of this phenomenon, called derivative kick in the literature, is the presence of zeros in the S-plane dominance region. And as a solution, this challenge presents the use of a reference filter, shown in **??** , which cancels the controller's zero and, subsequently, a structural change in the PI controller, making it what the literature calls I+P, which is basically placing the multiplied proportional part directly at the output, instead of the error, like shown in Figure 13. Both solutions promote the same effect, which is to alleviate the overshoot at the system output.

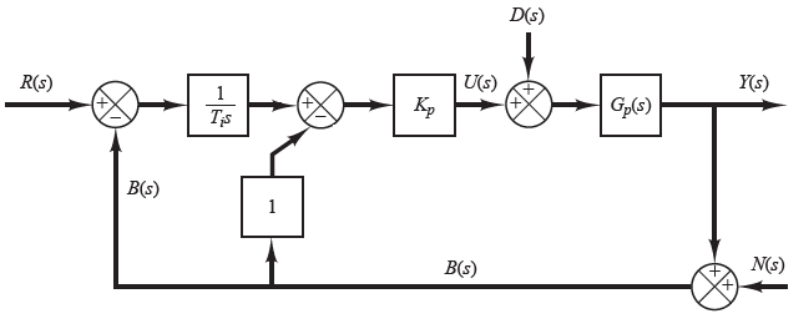

Figure 13: I+P controller applied to a system

Finally, the third problem addressed in this challenge is the Windup effect that occurs in some controllers when there is saturation in the control signal. Basically, some controllers suffer signal saturation due to physical limitation, either due to a reference beyond what the system can take, or due to a very abrupt disturbance . In these cases, the integral action causes the error to accumulate indefinitely, until a new reference is placed in the system or a disturbance takes the control signal to a feasible value. To solve this problem, some techniques called Anti-Windup are applied, in this case, the technique chosen was to turn off the controller's integrative action in the case of control signal saturation.

2.2 Simulations performed

The first step of Challenge II was to find an average model for the plant $G(s) = K_n \frac{e^{-sL_n}}{\tau_n s+1}$, where the parameters K_n, L_n and τ_n were determined by the arithmetic mean of four values previously determined by step response tests with different operating conditions, i.e. four plant models $G_1(s)$,$G_2(s)$,$G_3(s)$,$G_4(s)$ were determined by an identification method and each plant parameter was averaged, resulting in the nominal Plant:

$$G_n(s) = 1.05\frac{e^{-s0.65}}{1s+1} \tag{20}$$

Having determined a nominal model, the value of the modulus of multiplicative uncertainties was calculated, using **??**, for each of the four plants, in the frequency domain.

$$\Delta_i(\omega) = \left| \frac{G_n(j\omega) - G_i(j\omega)}{G_n(j\omega)} \right| \tag{21}$$

Then, varying the ω from 10^{-2} to 10^{-4} on a logarithmic scale, four graphs were generated for each multiplicative uncertainty. Once this was done, a Skogestad controller was designed , which is a PI given by:

$$C(s) = K_c \frac{sT_i + 1}{sT_i}$$

Where,

$$K_c = \frac{\tau_n}{K_n(\tau_c + L_n)}$$

$$T_i = min(\tau_n, 4(\tau_c + Ln))$$

With $\tau_c = 0.5$. Therefore, calculating the controller parameters, we obtained:

$$C(s) = 0.8282 \frac{s+1}{s} \tag{22}$$

Once the controller was designed, in order to analyze the robustness of the controller designed in Equation 22, a graph was generated of the product of the module of the complementary sensitivity function $|\mathcal{C}(j\omega)|$ by $\overline{\Delta}(\omega)$, where $\overline{\Delta}(\omega)$ is a vector with the maximum values of each multiplicative uncertainty, given by:

$$\overline{\Delta}(\omega) = max(\Delta_1(\omega), \Delta_2(\omega), \Delta_3(\omega), \Delta_4(== zzomega))$$

After all these calculations, five simulations were carried out to analyze the temporal response of the system in the configuration of Figure 1 with the designed controller 22. The first was done for the four models and considered:

$$F(s) = 1$$

$$R(s) = \frac{e^{2s}}{s}$$

$$Q_u(s) = 0.2 \frac{e^{25s}}{s}$$

$$Q_y(s) = 0$$

The next simulations were carried out only for the first model $G_1(s) = 1,3\frac{e^{-s0,9}}{1,2s+1}$, with some changes being made to the system. In the second simulation, only the reference filter was modified to $F(s) = \frac{1}{T_i s+1}$ with $T_i = 1$. In the third, the filter returned to being unitary, and the structure of PI was changed to I+P as shown in Figure 13. Maintaining this structural change and all other parameters, a saturation was added to the controller in the fourth simulation, defined by $u(t) \in [0, 0, 8]$. Finally, in the fifth and final simulation, considering all the changes made, an Anti-Windup action was added to turn off the integral action if the condition $|u_d(t) - u(t)| > 10^{-5}$ was met.

2.3 Results obtained

The first simulation result obtained in this challenge were the four graphs, Figure 14, Figure 15, Figure 16, Figure 17, of the modulus of multiplicative uncertainties as a function of frequency , with ω ranging from 10^{-2} to 10^{-4}.

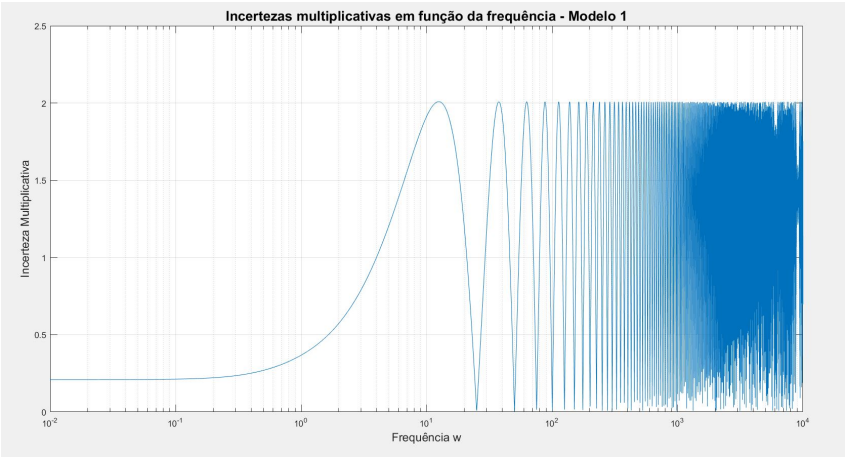

Figure 14: Multiplicative uncertainties as a function of frequency - Model 1

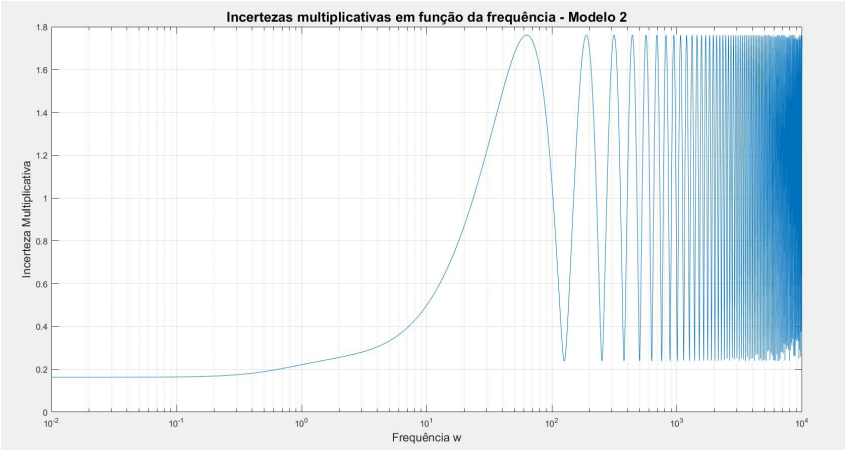

Figure 15: Multiplicative uncertainties as a function of frequency - Model 2

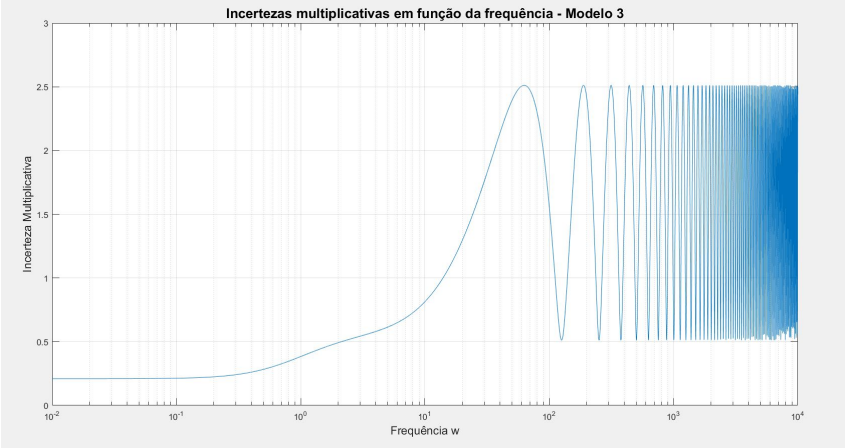

Figure 16: Multiplicative uncertainties as a function of frequency - Model 3

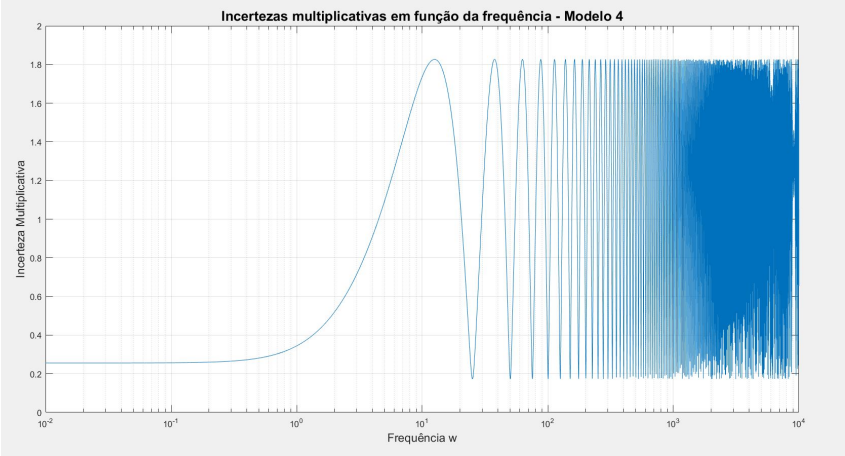

Figure 17: Multiplicative uncertainties as a function of frequency - Model 4

Where all models presented many noisy oscillations at high frequencies. Subsequently, the product graph $|\mathcal{C}(j\omega)|\overline{\Delta}(\omega)$ also depending on frequency, as shown in the figure below:

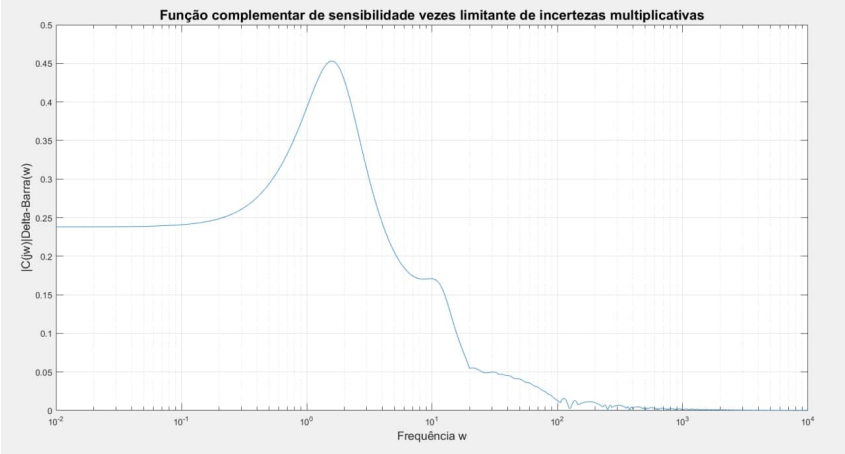

Figure 18: Product of the module of the complementary sensitivity function by the multiplicative uncertainty limit

In this case, the graph of Figure 18 guarantees that the controller $C(s)$ will provide robust stability for the four plant models considered, since all values of the product $|\mathcal{C}(j\omega)|\overline{\Delta}(\omega)$ are less than 1, obeying **??**.

Once the nominal plant was determined (20), the controller (22) implementing and the robust stability condition tested Figure 18, temporal simulation graphs were obtained as five different configurations. The first one was for the four models and with the conditions for $F(s)$, $R(s)$, $Q_u(s)$ and $Q_y(s)$ described in the Simulations section, obtaining:

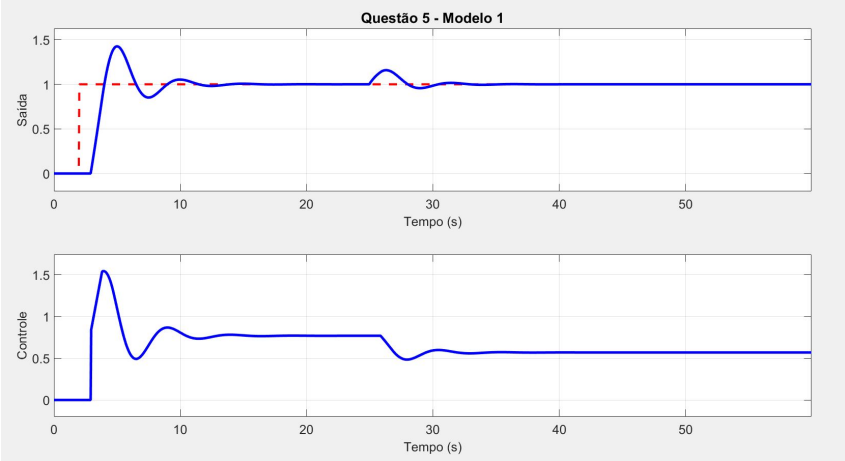

Figure 19: Model 1 Output and Control Signal

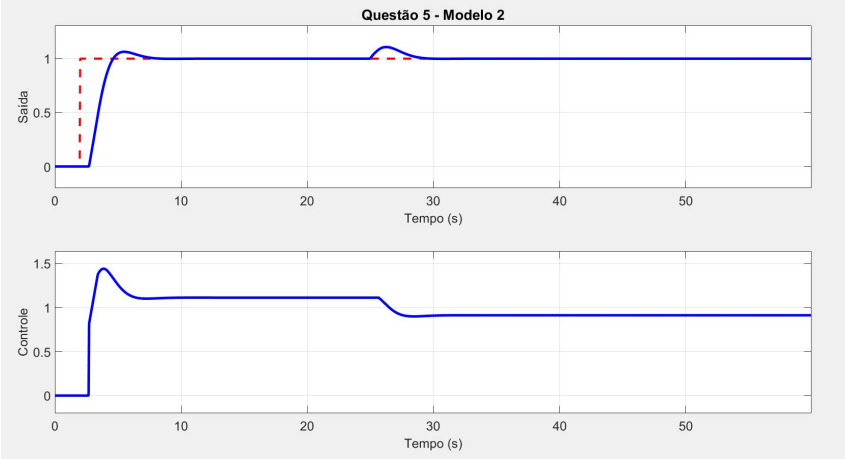

Figure 20: Model 2 Output and Control Signal

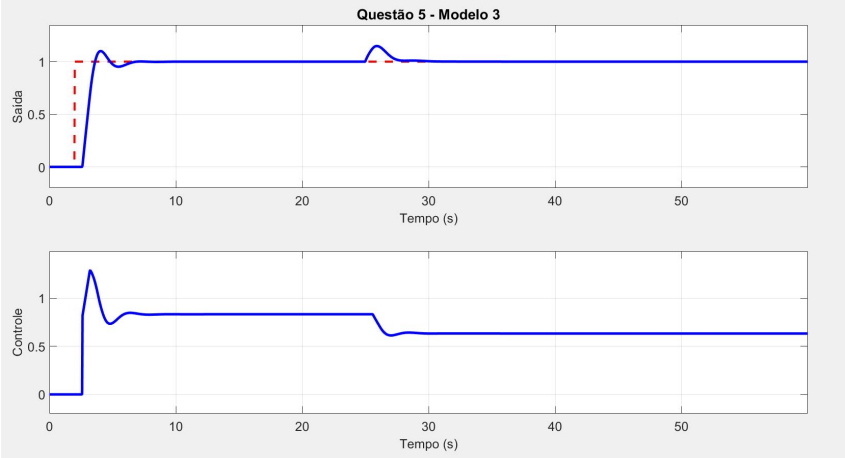

Figure 21: Model 3 Output and Control Signal

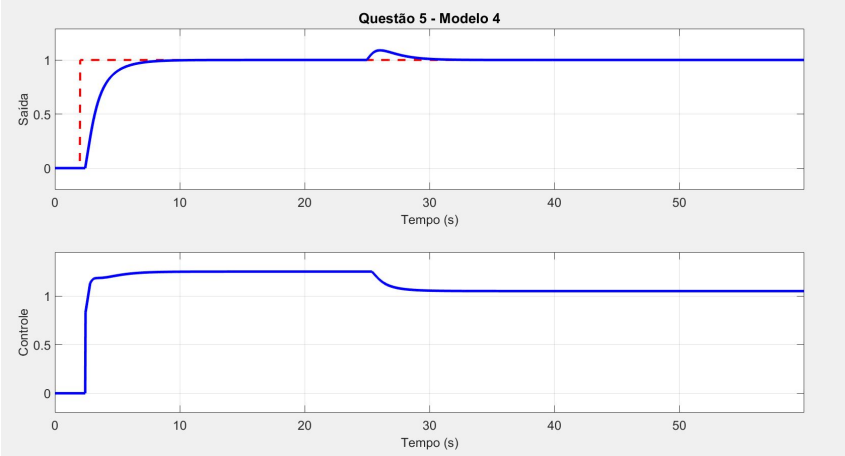

Figure 22: Model 4 Output and Control Signal

Where $Q_u(s)$ and $Q_y(s)$ had the temporal behavior shown in Figure 23 below:

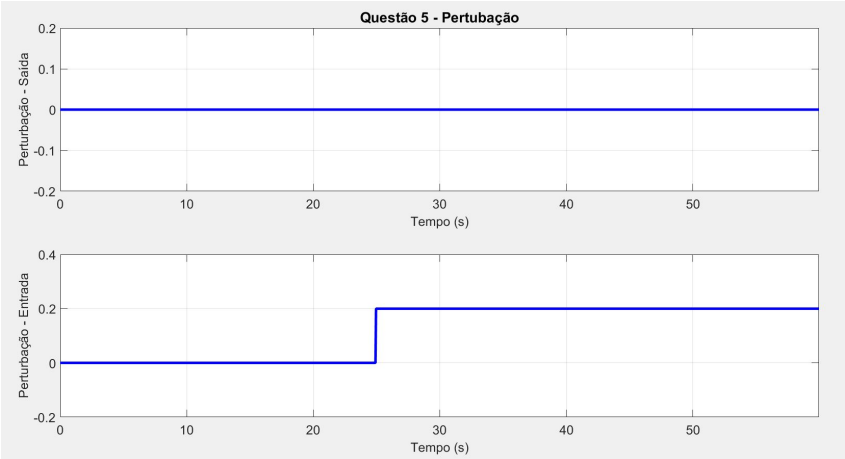

Figure 23: Disturbance Signal in $Q_u(s)$ and $Q_y(s)$

As theoretically expected, for all four cases, the controller was able to guarantee stability for the plant. Once this was done, modifying the reference filter, we obtained:

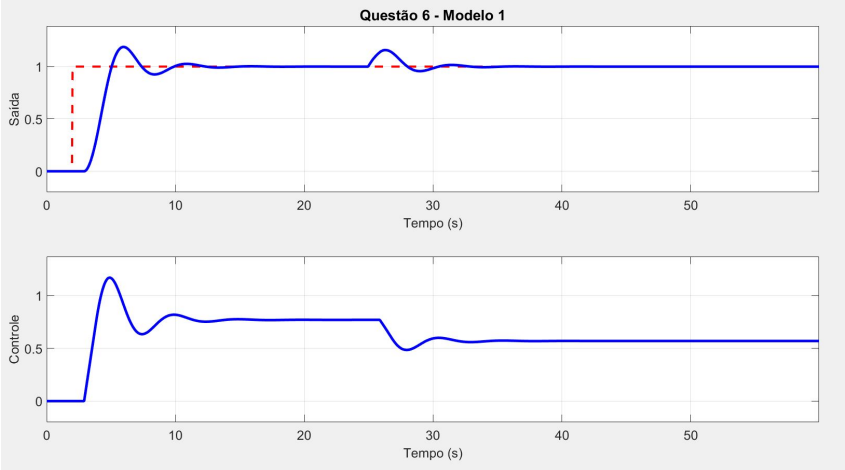

Figure 24: Model 1 Output and Control Signal with Reference Filter canceling controller zero

Subsequently, placing a unit value in the filter and reorganizing the mesh for an I+P control, we obtained:

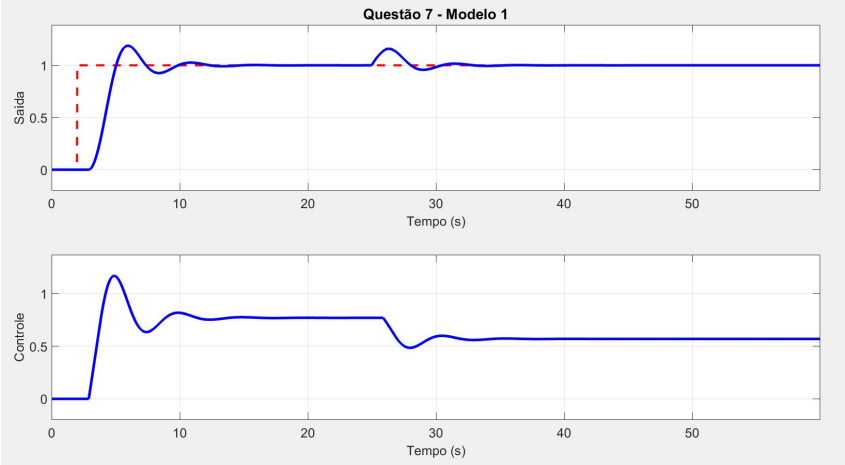

Figure 25: Model 1 Output and Control Signal with Unitary Reference Filter and I+P Controller

Therefore, when we compare the graphs in Figures 19, 24 and 25, we conclude that in question 5, the PI controller, due to the fact that it has a zero in the dominance region, causes a more pronounced overtone. And this problem - discussed in the Motivation section - is corrected by the Reference Filter canceling this zero from the PI controller Figure 24 and by changing the PI mesh structure, making it I+P. Both modifications produce the same result, since removing the proportional part of the direct path does not add a zero to the controller, for this reason, once the mesh is restructured, the reference filter is dispensed with.

As the last part of the challenge, a saturation in the control signal was implemented, generating the result below.

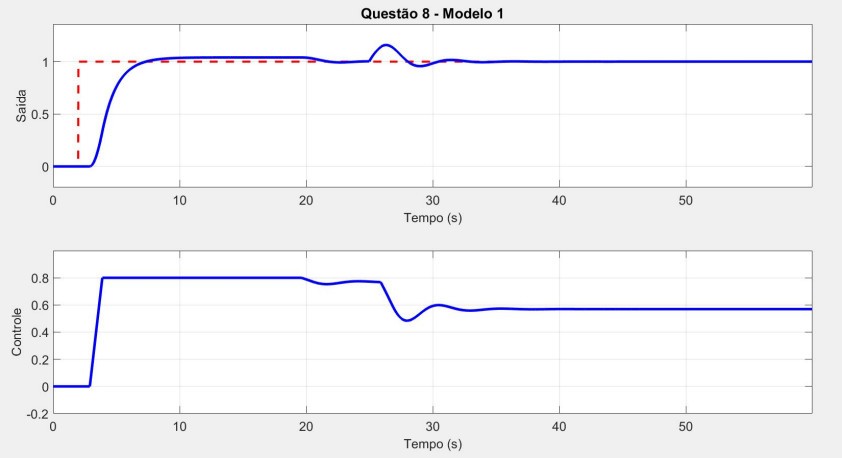

Figure 26: Model 1 Output and Control Signal with Control Signal Saturation

It can be seen that in this case, there is a shift in the reference segment from 8 seconds to 20 seconds, as there is an accumulation of the error integral in this period, due to controller saturation, characterizing the Windup effect . When this deaccumulation occurs, approximately after 20 seconds, the controller is able to bring the system to the reference. To fix this problem, an Anti-Windup full action shutdown action was implemented, obtaining the following simulation result:

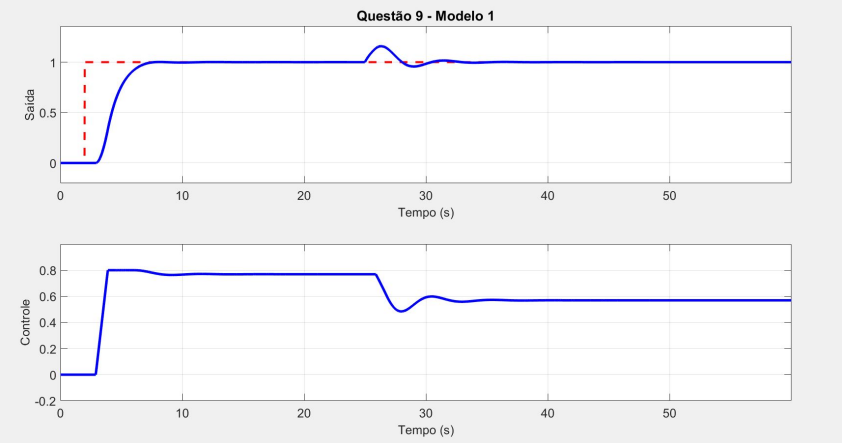

Figure 27: Model 1 Output and Control Signal with Control Signal Saturation and Anti-Windup Action

In the latter case, it can be seen that turning off the integrator does not allow the control signal to accumulate significantly, so the system reaches the reference at approximately 8 seconds.

2.4 Conclusions

It can be seen in the simulations carried out that both the small gain theorem, the use of a reference filter or mesh restructuring for an I+P controller and the action of turning off the integrator if there is saturation in the controller are four very efficient techniques. to solve the problems described in the motivation section. Robust stability was ensured, derivative kick was alleviated at the system exit and the Windup phenomenon was corrected.

3 Frequency Response

3.1 Motivation

When developing controller designs for dynamic systems, it is possible to work in both the time domain and the frequency domain. In this third and final challenge, phase advance compensator projects will be developed, Equation 23, based on the frequency response of the system considered. This control strategy proves to be effective and popular for some Power Electronics applications such as power converter designs and vibratory mechanical system designs. Following this strategy, the entire controller design is developed based on the system's open-loop transfer function, observing the effects caused in closed loop. Therefore, it is not necessary to assume modal dominance when sizing the parameters. Furthermore, it is worth mentioning that in some applications frequency analyzers are used to generate diagrams such as *Bode*, *Nyquist* and *Smith* Chart . Therefore, the phase advance compensator designs developed here will modify the transient part of the systems based on the phase and gain margins and their respective frequencies.

$$C(s) = K_c \frac{Ts+1}{\alpha Ts+1} \tag{23}$$

3.2 Simulations performed

For this work, the following transfer function for the process plant was considered:

$$G(s) = \frac{0,5}{(s^2+0.6s+1)(0.1s+1)} \tag{24}$$

$overline K$ was determined such that $\overline{K}G(0) = 1$, obtaining $\overline{K} = 2$. Subsequently, using the function *bandwidth( )* from *MATLAB*, the bandwidth of $P(s)$ was calculated, given by $P(s) = \overline{K}G(s)$, finding a frequency of $\omega = 1.4476\ rad^{-1}/s$. From then on, the phase advance controller projects began. The first brought as design requirements a gain $K_c = 1$, a phase margin of 60º and a bandwidth of $2.5\ rad^{-1}/s$. For this, the following algorithm in *MATLAB* was implemented to determine the parameters α and T:

1. Calculate the Function $G_1(s)$, where $G_1(s) = K_c P(s)$.
2. Use the function *margin ($G_1(s)$)* in order to return the value of the Phase Margin (γ) of $G_1(s)$.
3. Calculate maximum phase advance angle:

   $$\phi_m = \theta + \gamma + \varphi$$

   Where θ is the desired phase, which in this case is 60º, and φ is the clearance, which in this case is 12º.
4. Determines the alpha value by the equation:

   $$\alpha = \frac{1 - sin\phi_m}{1 + sin\phi_m}$$

5. Calculate the compensated system $G_{comp}(s) = \frac{1}{\sqrt{\alpha}} G_1(s)$.
6. Obtain the gain crossover frequency of the compensated system ω_{cp} again through the function *margin ( )*.
7. Calculate the value of $T = \frac{1}{\omega_{cp}\sqrt{\alpha}}$.
8. Thus determining the transfer function of the advance controller:

   $$C(s) = K_c \frac{Ts+1}{\alpha Ts+1}$$

After following the algorithm above, the open-loop frequency response of the system was obtained. The second controller was designed considering the same criteria above and the same algorithm, differing only in the clearance value φ which in this case was 24º. Then, in question 5, the value of the modulus of the open-loop transfer function was determined to the value of $\omega = 2.5$ and a value of K_c was determined such that the bandwidth reached up to $2.5 rad^{-1}/s$. This determination of K_c was done by the following command in $Matlab$:

» syms kc

» FTma = kc*(T*s+1)/((a*T*s+ 1)* Kb *G(s));
» Kc = solve(abs(FTma) == 1/sqrt(2));
» Kc = double(Kc)

Once this step was carried out, the next controller was designed following the algorithm described with a gap of 24º, but considering the new K_c determined above. After designing these three controllers, two temporal simulations were carried out for the system da Figure 1 with $F(s) = \frac{1}{Ts+1}$, $Q_u(s) = Q_y(s) = 0$ and G(s) given by Equation 24: one for the controller of Item 4 with a clearance of 24º and gain $K_c = 1$ and another for the controller of Item 6 also with 24º clearance and gain K_c determined by the *Matlab* commands described above. Then, the term below was added to the two controllers designed in Item 4 and 6.

$$\frac{\beta(T_{\alpha t}s + 1)}{\beta T_{\alpha t}s + 1}$$

Where $T_{\alpha t} = 5T$ and β was calculated for each case forcing the condition of $C(0)G(0) = 5$. Finally, two last simulations were carried out in the Figure 1 system with the two controllers modified by the term above. In the latter case, the simulation time was 200 seconds, the reference signal was $R(s) = \frac{e^{-2s}}{s}$, the disturbance at the output was zero and the disturbance at the input given by $Q_u(s) = \frac{e^{-120s}}{s}$

3.3 Results obtained

The results of the simulations described above begin with the determination of:

$$\overline{K} = 2$$

Subsequently, the bandwidth value of $P(s)$ was one:

$$\omega = 1.4476\ rad^{-1}/s$$

From there, the first controller designed in item 3 for a phase margin of 60º and clearance of 12º has the following transfer function:

$$C_3(s) = \frac{1.093s + 1}{0.3834s + 1} \tag{25}$$

Generating the following frequency response:

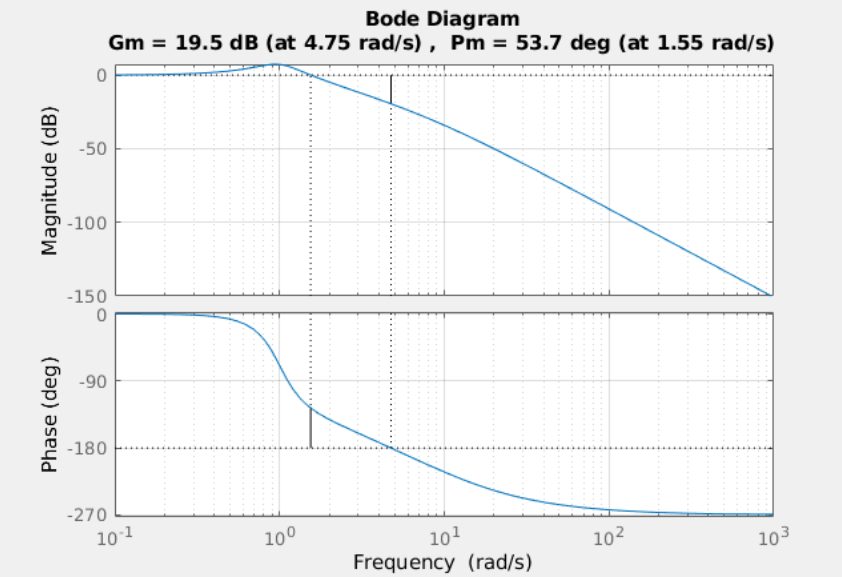

Figure 28: Item 3 Controller Frequency Response

However, through this simulation it is clear that the phase margin achieved was 53.7º, not reaching the design requirement of 60º, and the bandwidth achieved was $\omega = 1.8130$, also not meeting the criterion that was greater than 2.5 rad^{-1}/s. To achieve this, the second controller was designed with a clearance greater than 24º, resulting in:

$$C_4(s) = \frac{1.282s + 1}{0.2698s + 1} \tag{26}$$

And a frequency response :

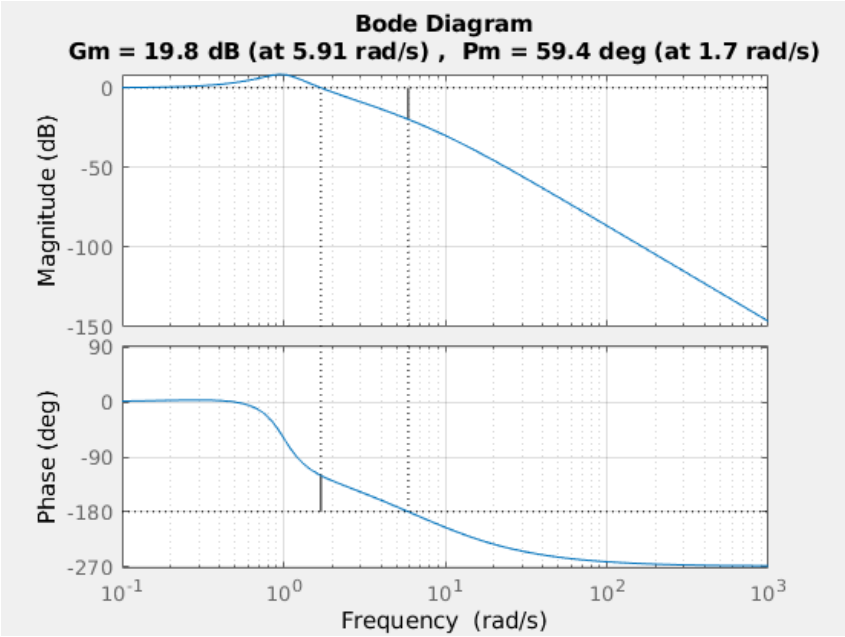

Figure 29: Item 4 Controller Frequency Response

Therefore, given the above result, it can be concluded that the new gap of 24º was necessary and sufficient to reach the phase margin of practically 60º. However, the bandwidth achieved was 2.05 rad^{-1}/s, still not meeting the 2.5 rad^{-1}/s criterion. In this way of meeting the performance criteria, the value of the gain of the mesh transfer function for $\omega = 2.5$ was obtained through the *bode* diagram , finding a value of -6, 14 dB. Subsequently, using the function *solve( )* of *MATLAB*, the value of the gain K_c was calculated such that the bandwidth was 2.5, obtaining:

$$K_c = 1.4297$$

With this new gain value, the phase margin value was increased to 64.3º. Continuing the challenge, the K_c above was fixed , the advance controller was redesigned in item 6, reaching the result:

$$C_6(s) = \frac{1.96s + 1.43}{0.143s + 1} \tag{27}$$

Which brought the following frequency response:

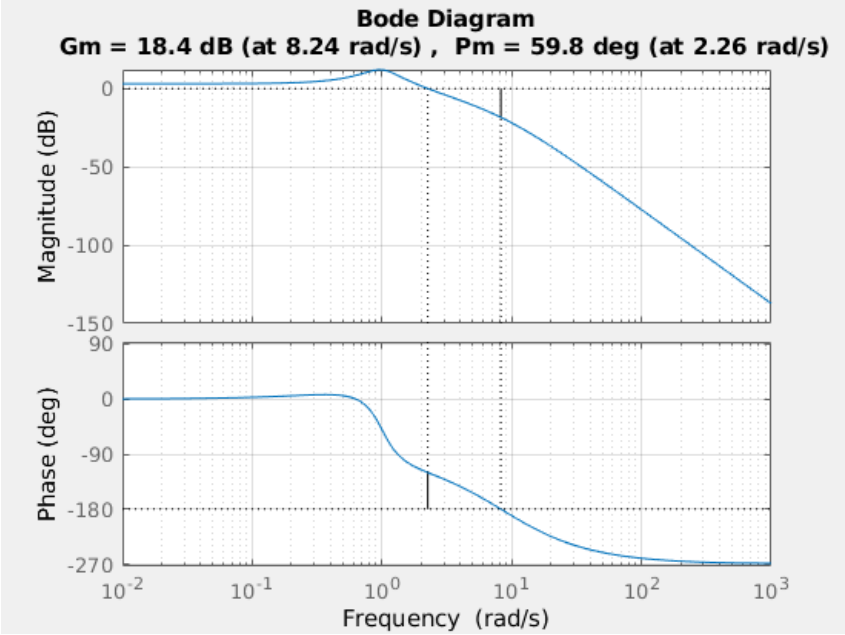

Figure 30: Item 6 Controller Frequency Response

And a bandwidth of 2.2412 rad^{-1}/s, therefore being the controller that came closest to the pre- established performance criteria. Next, the temporal response of the controllers in item 4 and 6 was simulated following the specifications described in the Simulations Section, obtaining for the C_4 controller:

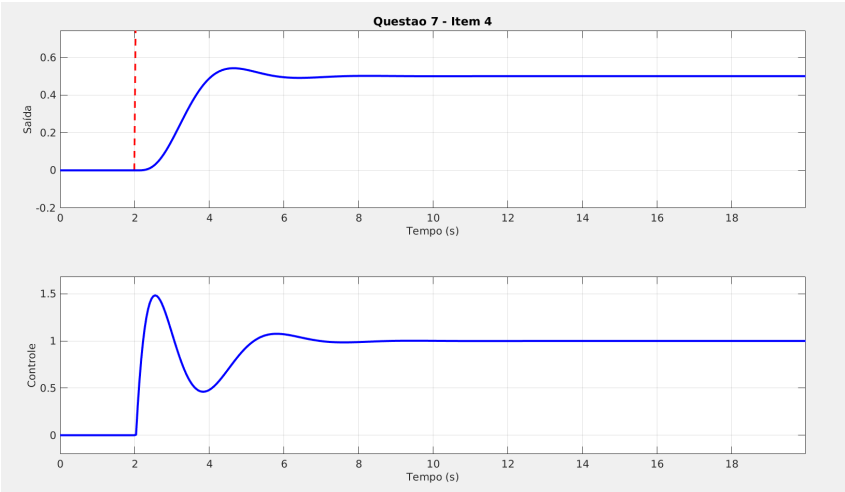

Figure 31: Item 4 Controller Temporal Response

And for the C_6 controller:

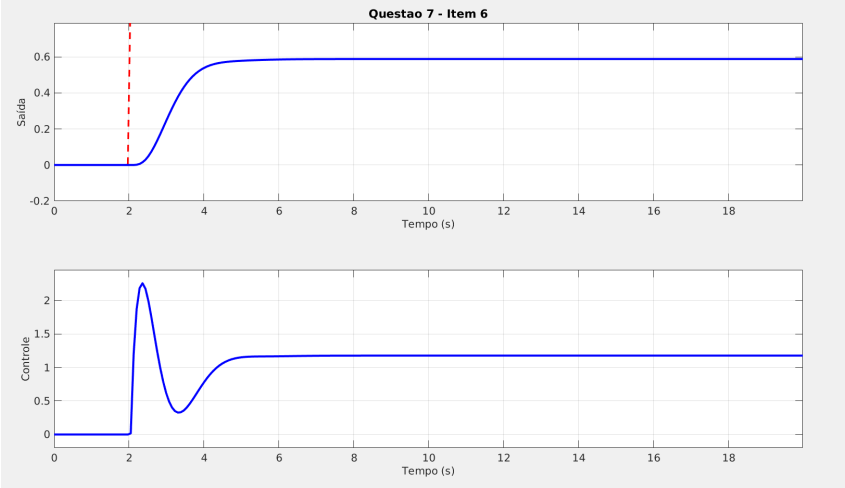

Figure 32: Item 6 Controller Temporal Response

Given the results of the temporal simulations, it is firstly concluded that in both results the phase advance controller acts on the transient part, as theoretically expected, observing a *offset* in the output signal in relation to the reference. However, when comparing the two figures 31 and 32, we also notice that the output of item 6 has a shorter settling time than that of item 4, which was also expected theoretically, since that the C_6 controller was designed to provide the open-loop transfer function with greater bandwidth . For the eighth question of the challenge, the following values of β were obtained for Items 4 and 6:

$$\beta_4 = 5.0000 \quad \text{and} \quad T_{\alpha t_4} = 6.4100$$

$$\beta_6 = 3.4965 \quad \text{and} \quad T_{\alpha t_6} = 6.8555$$

Thus designing the following modified controllers:

$$C_{4_{mod}}(s) = \frac{9.5033(s+0.78)(s+0.156)}{(s+3.706)(s+0.0312)} \tag{28}$$

$$C_{6_{mod}}(s) = \frac{27.413(s+0.7296)(s+0.1459))}{(s+6.993)(s+0.04172)} \tag{29}$$

Once the transfer function of the new controllers was determined, the system was temporally simulated with a reference filter and input disturbance as described in the Simulations section, obtaining the following answers:

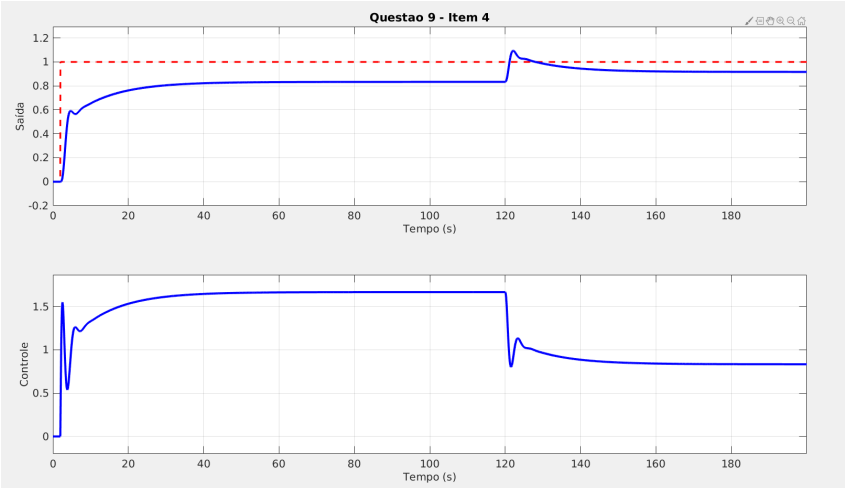

Figure 33: Modified Item 4 Controller Temporal Response

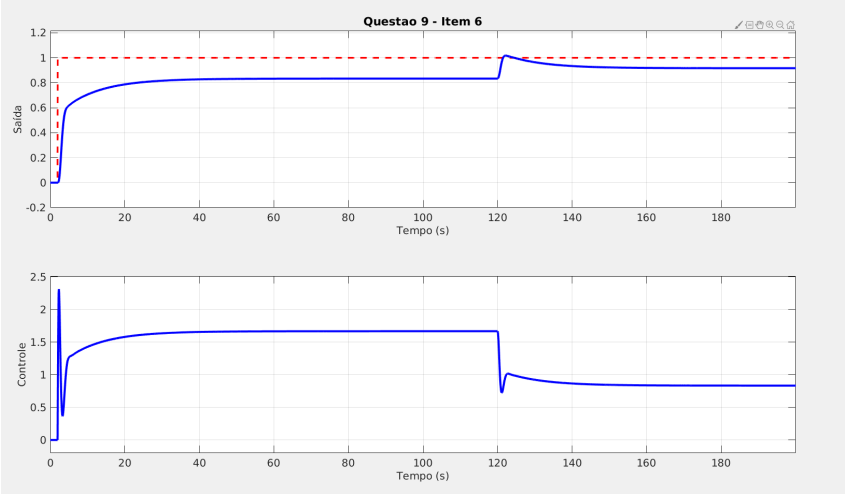

Figure 34: Modified Item 6 Controller Temporal Response

In these last simulations it is observed that the output of both items comes closer to the reference signal with the addition of the term in the controllers, making the outputs almost reach the unit value after disturbance rejection . Once again, it can be seen that the controller in item 6 rejects the disturbance faster than the controller in item 4.

3.4 Conclusions

In view of the projects and simulations carried out frequently in this present challenge, it appears that the execution procedure for these has much greater flexibility than is apparent in many literatures, which feature fixed and ready-made algorithms. Manipulation of phase margin, gap addition, controller gain and bandwidth settings allow the designer to control plants in various applications using this frequency domain strategy.